HIGH-RESOLUTION RADAR WAVE AND CURRENT MEASUREMENTS IN HIGHLY INHOMOGENEOUS COASTAL AREAS

Katrin Hessner[1], Konstanze Reichert[2], and Jose Carlos Nieto Borge[3]

[1] OceanWaveS GmbH, Lueneburg, Germany, hessner@oceanwaves.de

[2]OceanWaveS , Lower Hutt, New Zealand;

[3] University of Alcalá, Spain

Keywords: Remote sensing, nautical radar, high resolution waves, high resolution current fields, shallow water bathymetry

1 INTRODUCTION

Coastal waters are characterised by complex wave fields that are influenced by inhomogeneous bathymetries, and changing tidal and wind induced currents. The understanding of these interactions has gained more interest over the last years, especially for port entrances and close to shore shipping activities, and from the coast environmental perspective. In contrast to in-situ measurements, remote sensing techniques have the advantage to provide area covering data of several parameters (waves, currents and bathymetry), observed at the same time.

The wave and current monitoring system WaMoS II is a remote sensing system based on a nautical X-Band radar generally used for navigation and ship traffic control. Nautical radars are designed to monitor targets on the sea surface continuously over a relative large area (~ 10 km^2) with high spatial (~7.5 m) and temporal resolution (~2 s). Under various conditions, signatures of the sea surface itself become visible in the near range (less than 3 nautical miles) of nautical X-band radar images. These signatures include spatial and temporal information of the sea surface waves (wind sea and swell), hence nautical X-Band radar images can be used for sea state measurements Young et al., 1986; Nieto Borge et al., 1998; Reichert et al., 1998; Hessner et al., 2001). In recent years more focus was put on retrieving current and wave data at that high resolution on an operational basis (Hessner et al., 2007; Hessner and Bell, 2009).

In this paper a brief introduction into the high resolution current and water depth measurement principle of WaMoS II will be given. Data comparisons will be shown from the South Coast of New Zealand. The site is characterised by strong prevailing tidal currents as well as very inhomogeneous wave and current fields. In addition, the bathymetry changes strongly on a small spatial scale, which can be seen in both the current and the wave fields. The analysis will support the evaluation of areas in the ocean where consecutive high waves are traveling together, and how they propagate and change in time and space. Therefore, wave and current fields for three characteristic tidal states are presented. Further, time series of the currents are compared to model hindcast data for this area. For visualisation of the modification of the wave and current fields due to coastal effects, wave spectra and current figures for different locations are presented.

2 THE WAMOS II SYSTEM

WaMoS II is a high-speed video digitizing and storage device that can be interfaced to any conventional navigational X-band radar and includes a software package running on a standard PC. The software controls the radar, data analysis and storage, as well as the display of measurement results.

A WaMoS II wave measurement consists of the acquisition of a radar images and the subsequent wave analysis. For the wave analysis the spatial and temporal sea clutter information is transformed into the spectral domain by means of a three dimensional Fast Fourier Transform (FFT). Besides the directional unambiguous sea state information, the information of surface current, and in shallow water the water depth can be derived (Young et al., 1998, Senet et al., 2001). The standard WaMoS II software delivers in real time unambiguous directional wave spectra and time series of the integrated standard wave parameters: significant wave height (H_s), peak wave period (T_p), peak wave direction (θ_p) and peak wave length (λ_p). This data can be made available to the user on the WaMoS II PC and can also be transferred to other stations via Internet, LAN, NMEA etc.

Recent developments also allow monitoring operational current and wave fields, as well as local water depth in shallow seas. The measurement principle behind this is that the local propagation speed of waves (celerity) is effected by the water depth and the current. The relation between wave celerity and water depth and current is described by the *dispersion relation*. In shallow waters (water depth of less than half the wave length) the celerity of waves decreases with decreasing depth. This yields to coastal effects like wave shoaling and wave defraction. In the presence of a current, the wave also experiences an acceleration (positive when traveling with the current and negative when traveling against the current). This effect is known as the Doppler Effect. These effects allow WaMoS II to retrieve water depth and current from simultaneous wave observations in time and space. This principle was applied in the 1940s to remotely map coastal bathymetry for amphibious landing by means of arial images (Hard and Miskin, 1945).

Nautical X-Band radars allow to monitor waves at different ranges and various directions, and thereby give the ability to observe wave fields simultaneously in time and space. Hence it also delivers the possibility to obtain the wave included information on the current and bathymetry in time and space (Hessner et al., 1999; Bell, 2005; Hessner et al., 2007; Hessner and Bell, 2009).

3 WAMOS II STATION MAKARA

In a field experiment at Makara, New Zealand, WaMoS II measurements were used to derive current and wave fields. This station (41°20.4’ S 174°39.646’ E) is located near Wellington, at the South coast of Northern island of New Zealand (Figure 1).

In this area, the current field is characterized by a semidiurnal tidal current along the shore. Near the shore, a strong current shear parallel to the shoreline, can be observed. The wave field is characterized by long swell coming from the south – south west, interacting with the local bathymetry and the tidal current. Due to different coastal processes like wave shoaling, wave reflection and defraction, waves and current are highly variable in time and space.

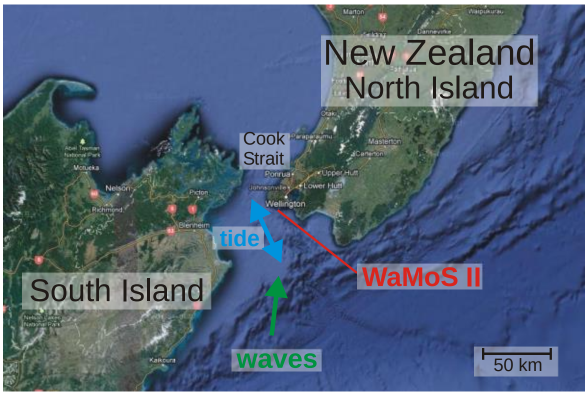

Figure 1: Google-map of the Cook Strait, New Zealand. The location of the WaMoS II station is marked red, blue indicates the main tidal current direction and green the dominant prevailing wave direction.

For the radar measurements a Decca Bridgemaster marine X- band radar with an 8 foot antenna with an radar repetition rate of RPT = 2.3 s was temporarily deployed about 20 m above sea level. The antenna has a tangential resolution of approximately 1°. The continuously sampled radar images were in the range of 560 m – 4400 m, with a radial resolution of 7.5m.

Figure 2 shows a WaMoS II radar image of the Makara site. In this example the maximum radar return is obtained from land targets related to the cliff land structure with steep peaks and valleys. The radar return from the sea surface (green-blue) shows wave pattern associated with the prevailing sea state / waves. Due to interaction of the waves with the local bathymetry and current, the wave pattern are variable in the observation area.

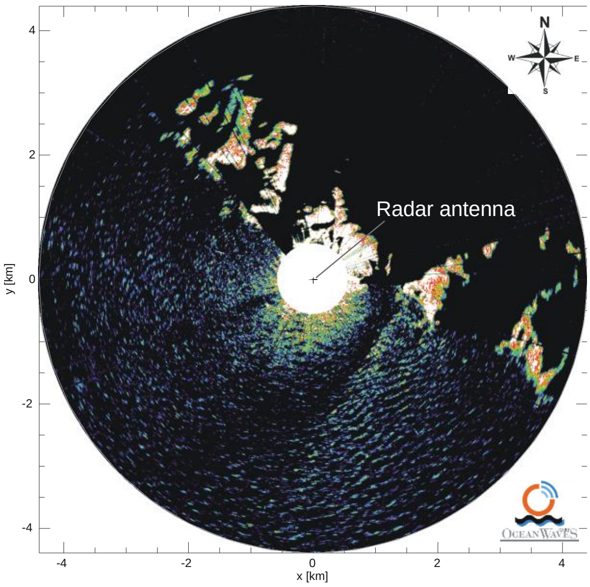

Figure 2: WaMoS II radar image acquired at Makara station Aug. 14th, 2011, 0:00 local time. The color is related to the radar backscatter strength from black (no radar return) to white (maximum radar return).

4 HIGH RESOLUTION CURRENT AND BATHYMETRY ANALYSIS

In the following discussion, WaMoS II data from Aug 14-16, 2011 is presented for three characteristic current scenarios: *high tide*, *slack tide* and *low tide*. For all three scenarios, a radar image showing wave patterns and associated wave fields, and the corresponding WaMoS II HRC bathymetry and current fields are presented. White areas are off the radar view or where the sea state / wave length is to low to retrieve reliable water depth other than the set up water depth of 50 m.

The presented data was analysed on a 39x39 grid with a spatial resolution of 225m. For the HRC analysis a sequence of N = 32 images were used, so that the resulting measurements represent a temporal mean of 73.6 s.

4.1 HIGH TIDE

Figure 3 shows a WaMoS II radar image of a high tide scenario. The image was obtained on August, 15th, 2011, 7:01 UTC.

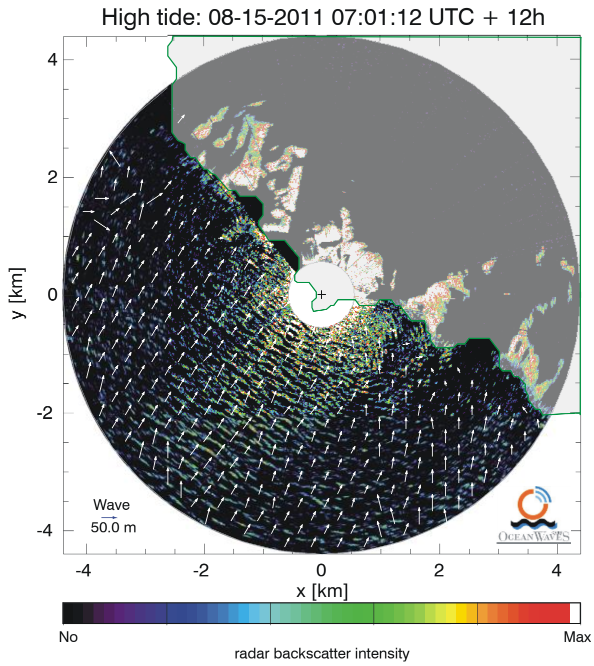

Figure 3: WaMoS II radar image as obtained at Makara during *high tide*: Aug. 15th, 2011, 7:01. The color indicates the radar backscatter intensity. The white arrows indicate the peak wave direction of the incoming waves.

At that time the tidal current is maximal oriented northwest-ward.

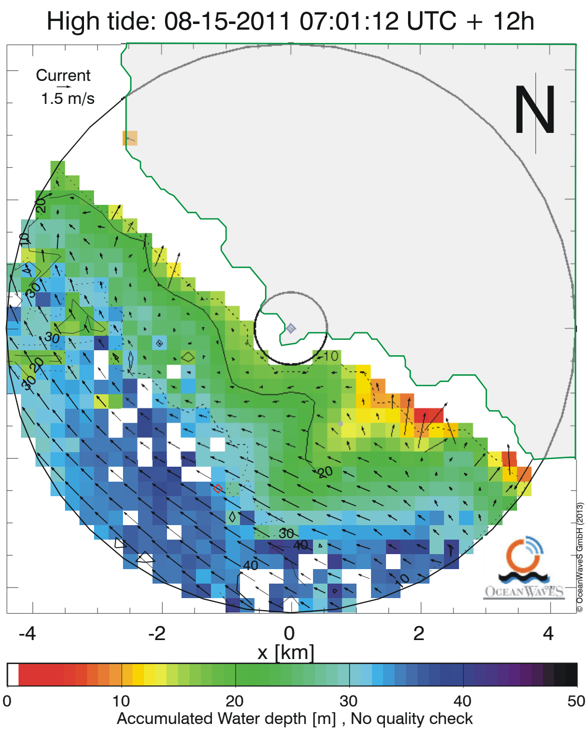

Figure 4: Bathymetry and current field as obtained by WaMoS II HRC at Makara during *high tide*, Aug. 15th, 2011, 7:01. The color represents the HRC water depth, the arrows the current vectors.

The observed wave field is almost homogeneous with waves approaching the coast from southwest. The obtained HRC peak wave vectors are overlaid as white arrows. Near shore, south east of the radar antenna, an area with perturbations in the wave field due to coastal effects can be observed. There, the stripe like wave signature changes its orientation. The associated wave vectors indicate different wave propagation directions in this area.

The WaMos II HRC depth (Figure 4) retrieval yields a bathymetry with water depth deeper than 30 m off the coast (> 3 km). Near shore, a reef structure (ca. 2 km south east of the antenna) aligned perpendicular to the shoreline with a minimum water depth below 10 m is visible. In this area the retrieved water depth ranges from 10m-15m and significant disturbance in the wave and current field can be observed. With increasing water depth and distance to the shore, the current speed increases up to 2 m/s. Off the coast, in water depth > 30 m, the current is almost homogeneous.

4.2 SLACK TIDE

Figure 5 shows the WaMoS II radar image as obtained at the proceeding slack tide.

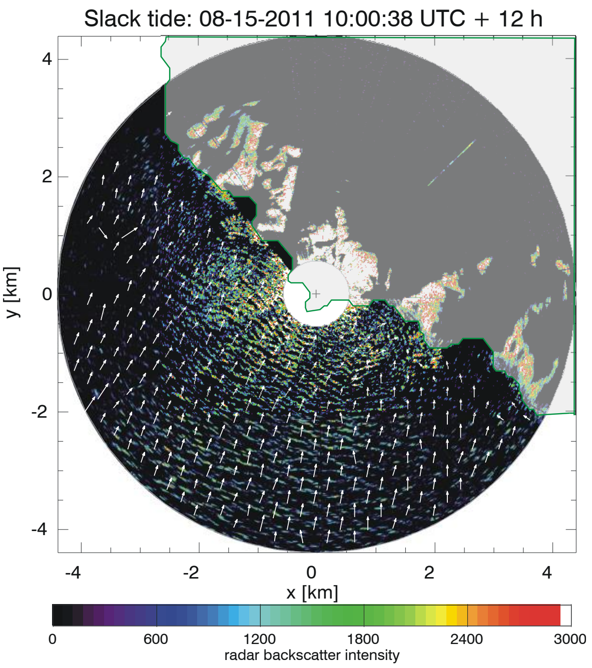

Figure 5: WaMoS II radar image as obtained at Makara during *slack tide*: Aug. 15th, 2011, 10:00. The color indicates the radar backscatter intensity. The white arrows indicate the peak wave direction of the incoming waves.

The observed wave field did not visually differ significantly from the wave field at *high tide*. Wave are approaching from the southwest with disturbances southeast of the radar antenna.

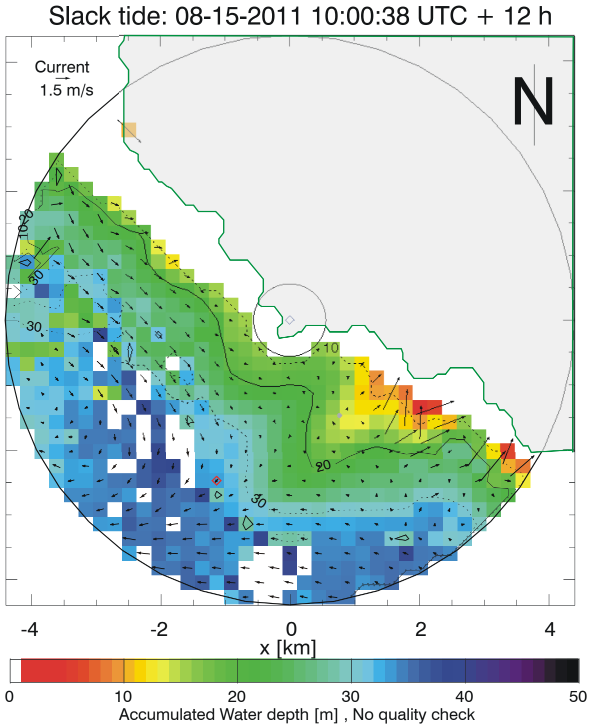

Figure 6: Bathymetry and current field as obtained by WaMoS II HRC at Makara during *slack tide*, Aug. 15th, 2011, 10:00. The color represents the HRC water depth, the arrows the current vectors. The red diamond indicate the location for which the time are shown in Figure 9.

In contrast to the wave field, the obtained HRC current field (Figure 6) shows a significantly different pattern than at *high tide*. This time, the overall current speed is low and varies in space significantly. In the western part of the observation area a clockwise rotating eddy structure can be observed with its centre at the western edge of the WaMoS II radar observation area. Southwest of the centre of the eddy, a convergent current zone can be observed.

4.3 LOW TIDE

In Figure 7, the WaMoS II radar image as obtained during low tide Aug. 15th, 2011 13:00 is shown. Again, the wave patterns show no significant difference to the high or slack tide cases.

Again, an almost homogeneous wave field with perturbations at the reef southeast of the radar

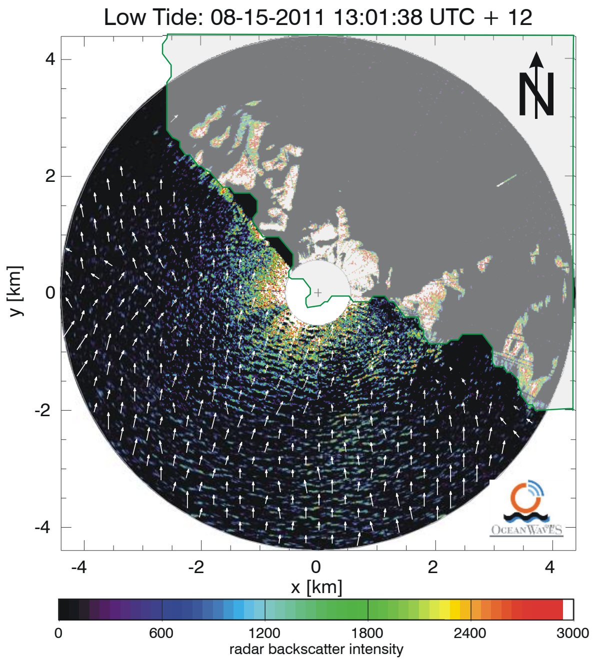

Figure 7: WaMoS II radar image as obtained at Makara during low tide: Aug. 15th, 2011, 13:01. The color indicates the radar backscatter intensity. The white arrows indicate the peak wave direction of the incoming waves.

antenna are visible. In this area the observed wave field is characterized by two wave systems propagating in different directions.

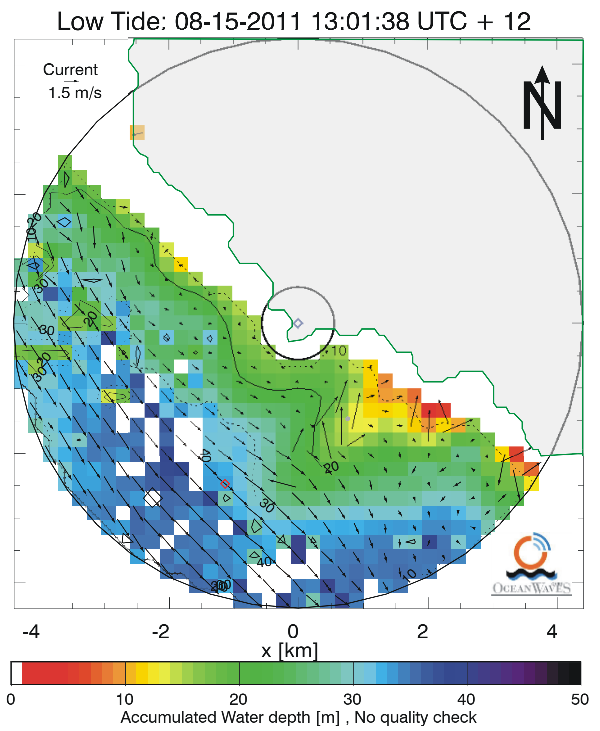

Figure 8: Bathymetry and current field as obtained by WaMoS II HRC during *low tide*, Aug. 15th, 2011, 13:01. The color represents the HRC water depth, the vectors the current.

The observed current field (Figure 8) is almost homogeneously aligned along the coast in a southeast direction with maximum off shore current speeds of about 2m/s southeast of the antenna, a reef structure with water depth below 15 m is visible. This reef is oriented almost perpendicular to the general coastline and represents a flow barrier of the general current. Therefore, in this area unrealistic current speeds are observed. This is most likely related to nonlinear wave-current interaction or due to wave breaking at the reef.

4.4 VARIATION OF CURRENT IN TIME

Observations of the current at one point deliver information of temporal evolution of the current. Figure 9 shows the current speed (top) and current direction (bottom) as observed by WaMoS II at the observation point about 2 km south of the radar antenna (red). As reference, the current delivered by the RiCOM storm surge model obtained for the grid point latitude 41.3704° S and longitude 174.653° E, is shown in blue. The RiCOM storm surge model simulates the dynamics of the Cook Strait including Marlborough Sounds and Fiordland (Lane, Walters, Gillibrand, & Uddstrom, 2009). Note that the update rate of WaMoS II measurements are 3 minutes representing a 32x2.3s mean value, while the model data is updated every 1 hour.

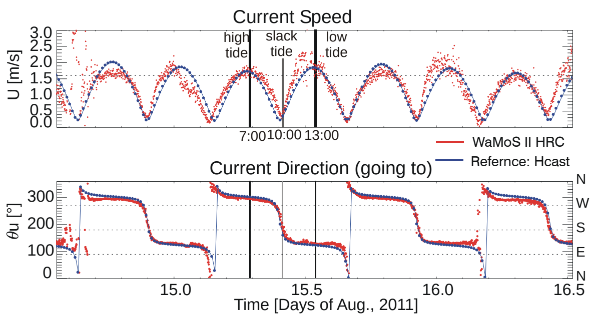

Figure 9: Time series of the current speed and direction as obtained by WaMoS II (red) and Hindcast model (blue) for Aug. 15th, 2013.

The WaMoS II, as well as the model data, shows that the current in this area is dominated by the semidiurnal M2 tide, with northwest-ward (~300°) flood and southeast-ward (~130°) ebb current. The vertical lines indicate the times of high, slack and low tides presented in Figure 3-9. Both, flood and ebb current have a magnitude around 1.5 – 2 m/s. Around slack tide, the current is rapidly changing its direction, with minimum current speed below 0.2 m/s. Compared to the model data, the measured WaMoS II HRC current data exhibits a natural variation. As they represent a 73.6 s mean value, the WaMoS II measurements include also short term current components related to wind, Stokes drift, buoyancy, etc. which are not covered by the model.

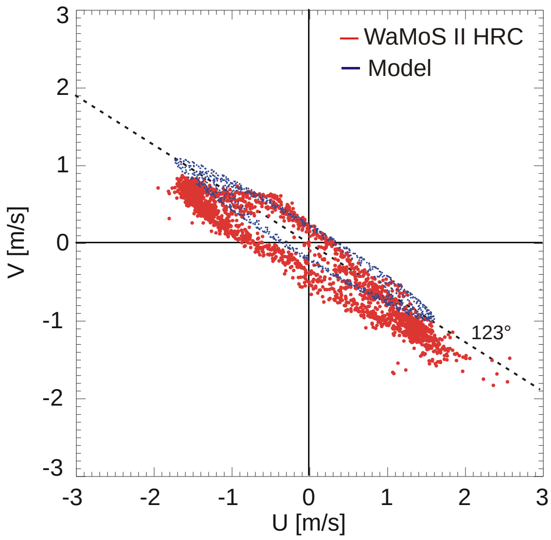

Figure 10: Current figure as derived from the WaMoS II HRC current measurements derived for Aug. 15th, 2011 at Makara (red) and the reference model (blue).

In Figure 10 the corresponding current figure of the WaMoS II HRC (red) and model (blue) are shown. It clearly exhibits the tidal ellipse which is oriented 123° along the main coast line. In contrast to the model which shows only the spring-neap tidal current variation, the WaMoS II current shows also a variation due to the coastal effects and non-tidal current components. This comparison indicates a south-eastward residual coastal current of 0.2 m/s.

4.5 VARIATION OF SEA STATE IN SPACE

As WaMoS II allows the observation of waves in space, it is possible to determine spatial variation of the sea state.

Figure 11 illustrates the modulation of the waves along two transects perpendicular to the shore. The red transect is located in relatively homogeneously decreasing water depth. The blue transect gives information along the reef with highly variable water depth and current. The HRC parameters (accumulated water depth, current, peak wave parameter) for the different observation points are summarized in Table 1.

Along both transects, wave shoaling with deceasing wave length can be observed. Along the red transect, the wave length decreases from 164.65m, off-shore (A), at a water depth of 39.12m to 119.07m , near shore (C), at 18.2 m water depth. The blue transect is located along the reef. Also along this transect waves shoal from off-shore (A) with a wave length of 151.79 m at 34.87 m water depth to near-shore (C) around 104.13 m at 20.46 m water depth. At the nearest coastal point (D), at a water depth of 15.17 m, a bi-modal sea state can be observed. One with a peak wave direction of 172.88° and a peak wave length of 119.07 m, and the other with 268.56° and 85.6 m. The first wave system is related to the incoming wave bended towards the reef. The second wave system can be associated with the waves reflected from the shore north of the observation point. There, the coastline is oriented about east-west hence the reflected wave propagate southward.

Table 1: HRC water depth, current and wave parameter as obtained for two coastal normal transects.

	Distance to Antenna	Angle relative to antenna	Estimated distance from shore	Accumulated water depth	Current speed	Current direction	Peak wave direction	Peak wave length
	R(radar) [m]	Φ(radar) [°]	R(coast) [m]	Adep [m]	U [m/s]	θu [°]	θp [°]	λp [m]
A	2869.1	225.0	~ 2500	39.12	1.49	148.7	210.96	164.65
B	1914.5	225.0	~1500	33.23	0.94	164.0	218.66	149.93
C	959.9	225.0	~ 500	18.20	0.31	171.5	209.74	119.07
A	3138.7	201.1	~ 3400	34.87	2.21	146.1	198.43	151.79
B	2299.0	191.4	~ 2400	27.87	1.77	152.9	218.66	149.93
C	1594.2	172.0	~ 1400	20.46	0.77	163.7	220.60	104.13
D	1272.8	136.2	~400	15.17	0.68	177.7	172.88	119.07
							268.56°	85.6

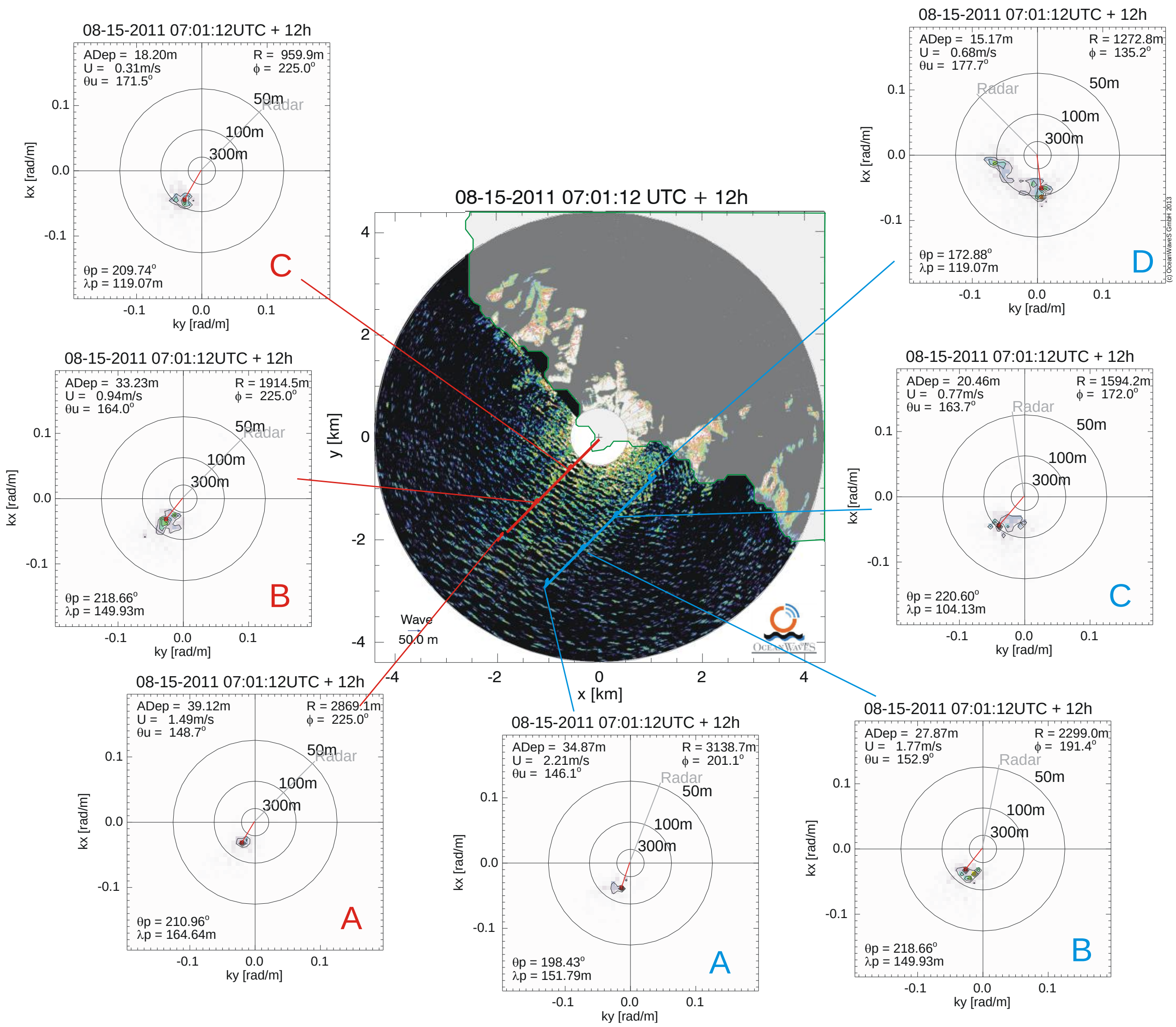

Figure 11: WaMoS II radar image and corresponding HRC wave spectra a obtained on two transects oriented parallel to the coast.

As the waves from the north (θp~172°) come from deeper water the corresponding wave length is longer compared to the waves approaching this area from west (θp~268°).

Figure 12 and 13 show the temporal evolution of the wave spectra for an off-shore location (A) and near-shore location (B). The colour is related to the normalized observed wave energy. The off-shore frequency spectrogram (Figure 12) shows a modulation related to the varying wave energy, with a maximum around 12 o'clock. At this time the wave spectrum has a broader frequency distribution. Nevertheless the peak frequency is almost constant. Only the peak wave direction shows a slight tidal modulation.

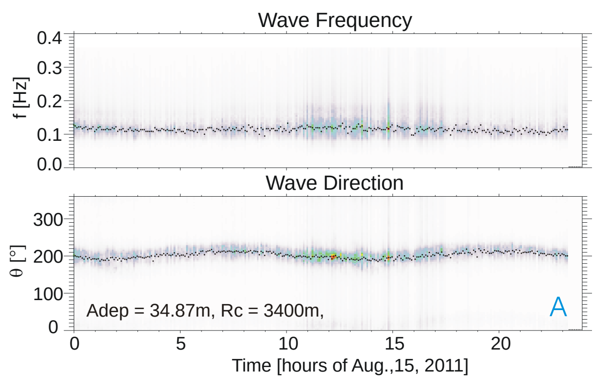

Figure 12: Frequency and direction spectrogram of the wave field as observed at grid point (A) about 3.4 km off shore with a water depth of 34.87 m.

The near shore spectrogram (Figure 13) shows a general broader energy distribution, with a temporary appearing second wave system around 260°. The primary, dominant wave direction is around 175° which represents the reflected waves. Hence it seems that the wave approaching from the west can reach this area only at decreasing flood current (high tide). During low tide (~13:00) almost no wave from west can be observed.

In the area and in general in the case of bi-modal seas, the derived peak wave direction is not able to represent sea states as it represents a mixture of the individual wave directions.

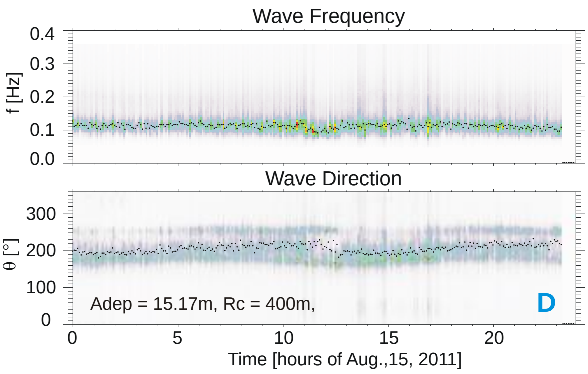

Figure 13: Frequency and Direction spectrogram of the wave field as observed at most near shore grid point (D) about 0.4 km off shore with a water depth of 15.17 m.

4.6 VARIATION OF CURRENT IN SPACE

Figure 14 shows a comparison between the observed WaMoS II HRC wave length, current speed and direction at different distances and different water depths from the shore in relation to the model data.

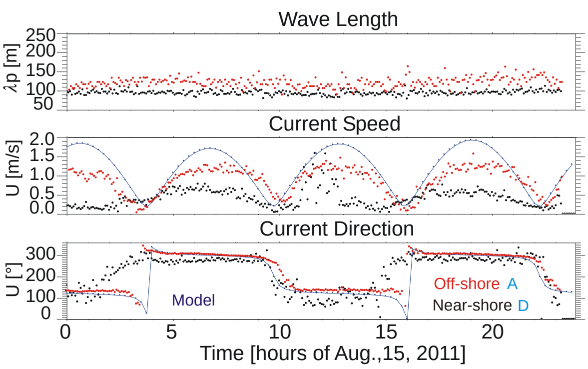

Figure 14: Time series of the HRC peak wave length, current speed and direction as obtained as the off- shore grid point (A, ~35m water depth red) and near shore grid point (D, ~15m water depth, black) and the model (blue).

Note that the numerical model is not capable of resolving all coastal processes which appear in this area. The comparison of the wave length reflects again the wave shoaling process, with shorter wave lengths in shallow water near the coast. Also, a lower current speed near shore is observed with tidal current magnitude of 1 m/s off-shore, and 0.6m/s at the near shore location. The current direction of the off-shore position shows good agreement with the model, while the near shore current direction exhibits a modulation due to the interaction with the local bathymetry.

Figure 15 visualizes the variation of the current in space due to local bathymetry. Off shore (positions A, B) tidal ellipses oriented along the general coastline with significant cross shore current components can be observed. With decreasing water depth (distance from shore), the tidal ellipses is modified. This modification is characterized in the first instant by a decrease in current speed. In addition, the ellipses are getting more deformed near shore with no cross-shore current components.

5 SUMMARY AND CONCLUSION

In this paper, spatial and temporal wave and current measurements by WaMoS II HRC at Makara, New Zealand during Aug. 2011, are presented. Wave and current fields are presented for characteristic times*: high, slack* and *low tide*. The measurements show the different current patterns with local variation in the wave and current fields due to the tides and the interaction with the local bathymetry. Aside from almost homogeneous dominant tidal current up to 2 m/s magnitude along the coast, the data allows the identification of small scale current features like eddy-like structures, convergent/divergent zones, as well as a coastal sheer zone, which is typical for this area. Furthermore, the spatial variation of the wave spectrum and the current along two transect aligned normal to the coast are presented. Along these transects, different modifications of the waves due to coastal effects were observed: Decreasing wave length with deceasing water depth due to wave shoaling, bending of wave direction due to defraction, and the generation of new wave systems due to reflection. Even though the current is dominated by the tides, the current shows significant modification by the local bathymetry.

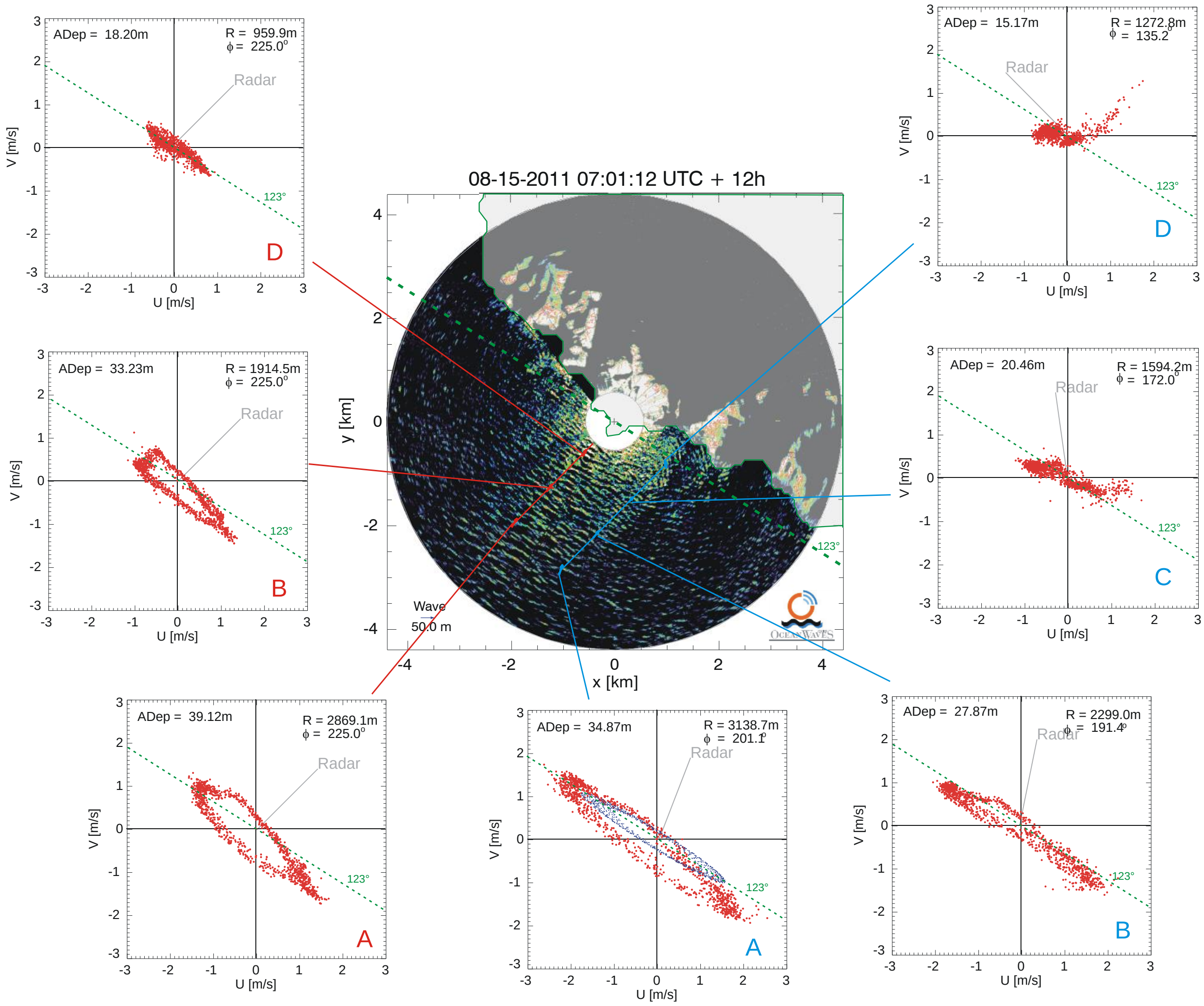

Figure 15: WaMoS II radar image and corresponding HRC current figure (red) as obtained on two transects oriented parallel to the coast. The blue tidal ellipse (A) refers to the model currents. The dashed green line indicate the orientation of model tidal current.

The observed tidal ellipses vary significantly in space.

The presented results show that in coastal areas with variable bathymetry the local hydro dynamic, waves and current, are not homogeneous, but can vary significantly in space. Hence to study hydro dynamic processes in those areas, individual points measurements are not sufficient.

6 ACKNOWLEDGEMENTS

The WaMoS II data was acquired within the ONR funded project Hi-Res (N00101411WX20493). The presented model data was kindly provided by NIWA (National Institute of Water & Atmospheric Research Ltd., New Zealand). The work presented here was co-funded in the framework of the Eu-Project DOLPHIN SPA.2010.1.1-05.

7 REFERENCES

Bell, P. S. (2005). Remote determination of bathymetric changes using ground based radar. *PhD thesis.*

Hart, C. A., & Miskin, E. A. (1945). Developments in the method of determination of beach gradients by wave velocity. *Air survey research paper No 15*, 1-54.

Hessner, K. G., & Bell, P. S. (2009). High resolution current & bathymetry determined by nautical X-Band radar in shallow waters. *Proc. of the OCEANS May 11-14, 2009*.

Hessner, K. G., Nieto-Borge, J. C., & Bell, P. S. (2007). Nautical Radar Measurements in Europe: Applications of WaMoS II as a Sensor for Sea State, Current and Bathymetry. In V. Barale, & M. (. Gade, *Sensing of the European Seas* (pp. 435-446). Springer.

Hessner, K. G., Reichert, K., & Rosenthal, W. (1999). Mapping of sea bottom topography in shallow seas by using a nautical radar. *Proceedings: 2nd Symposium on Operationalization of Remote Sensing*.

Hessner, K., Reichert, K., Dittmer, J., Nieto Borge, J., & Günter, H. (2001). Evaluation of WaMoS II Wave data. *WAVES 2001 conference, San Francisco September 1-6*.

Lane, E. M., Walters, R. A., Gillibrand, P. A., & Uddstrom, M. (2009). Operational forecasting of sea level height using an unstructured grid ocean model. *Ocean Modelling*, 88-96.

Nieto Borge, J., Reichert, K., Dittmer, J., & Rosenthal, W. (1998). WaMoS II: A wave and current monitoring system. *Proceed. Of the COST 714 conference on directional wave spectra, Paris.*

Senet, C. M., Seeman, J., & Ziemer, F. (2001). The near-surface current velocity determined from images sequences of the sea surface. *IEEE Trans Geosci Remote Sens 39 (3)*, 492-505.

Young, I., Rosenthal, W., & Ziemer, F. (1985). A three-dimensional analysis of marine radar images for the determination of ocean wave directionality and surface currents. *J. Geophys. Res.*, pp. 1049-1059.